CARBON 48 (2010) 3760–3768

available at www.sciencedirect.com

ScienceDirect

journal homepage: www.elsevier.com/locate/carbon

Computer simulation for storage of methane and capture of carbon dioxide in carbon nanoscrolls by expansion of interlayer spacing

Xuan Peng [a,b,*], *Jing Zhou* [c], *Wenchuan Wang* [d], *Dapeng Cao* [d]

[a] *College of Information Science and Technology, Beijing University of Chemical Technology, Beijing 100029, People's Republic of China*
[b] *Guangzhou Center for Gas Hydrate Research, Chinese Academy of Sciences, Guangzhou 510640, People's Republic of China*
[c] *Beijing Synchrotron Radiation Facility, Institute of High Energy Physics, Chinese Academy of Sciences, Beijing 100049, People's Republic of China*
[d] *Division of Molecular and Materials Simulation, Key Lab of Nanomaterials, Ministry of Education, Beijing University of Chemical Technology, Beijing 100029, People's Republic of China*

ARTICLE INFO

Article history:
Received 16 December 2009
Accepted 13 June 2010
Available online 17 June 2010

ABSTRACT

We perform a molecular simulation study on methane and carbon dioxide storage in carbon nanoscrolls. The effects of temperature and pressure, interlayer spacing, VDW gap and innermost radius on the gas storage have been examined extensively. It is found that the adsorption of gases on pristine carbon nanoscrolls is relatively low. However, once the interlayer spacing is expanded, both adsorption capacities of methane and carbon dioxide exhibit a significant improvement. In particular, the excess uptake of methane reaches 13 mmol/g at $p = 6.0$ MPa and $T = 298.15$ K and VDW gap $\Delta = 1.1$ nm, which is about 3.5 times of uptake of the pristine carbon nanoscrolls; while the uptake of carbon dioxide could also be raised by 294.9% at $T = 298.15$ K and $p = 3.0$ MPa and $\Delta = 1.5$ nm, reaching 30.21 mmol/g at 6.0 MPa. This work demonstrates that carbon nanoscrolls with an expansion of interlayer spacing may be a suitable material for methane storage and carbon dioxide capture.

1. Introduction

Nowadays, exhausted exploitation of fossil fuel in industrial process has been increasing the concentration of carbon dioxide in atmosphere and leading to more and more serious problem about global warming [1]. Carbon dioxide capture and storage (CCS) [2] thus becomes one of the most urgent and significant topics worldwide. On one hand, methane steam reforming reaction [3], which uses methane and water vapor as raw materials to produce hydrogen, is a major industrial source of carbon dioxide as a by-product. On the other hand, methane and carbon dioxide are the primary components in natural gas [4,5], except nitrogen and heavier hydrocarbons. The existence of carbon dioxide will reduce the energy content of natural gas and corrupt the transportation and storage system [1,4]. For the purposes of effective utilization of energy and sequestration of the greenhouse effect, removal of carbon dioxide from the resultant of methane steam reforming reaction or from natural gas is necessary for both cases. In the meantime, storage of methane is of equal importance as carbon dioxide. To achieve the above goals, adsorption technique using suitable porous materials is still a

* *Corresponding author at*: College of Information Science and Technology, Beijing University of Chemical Technology, Beijing 100029, People's Republic of China, Fax: +86 10 64427616.
E-mail address: pengxuan@mail.buct.edu.cn (X. Peng).
0008-6223/$ - see front matter
doi:10.1016/j.carbon.2010.06.038

prospective candidate for its high energy efficiency, low operating cost and ease of control over a relatively wide range of pressures and temperatures [1,4–6].

To date, a great deal of effort has been contributed to the development of novel porous materials and their applications in gas storage and separation, for example, metal–organic frameworks (MOFs) and covalent-organic frameworks (COFs) [7–12]. Even though, carbon-based materials are still preferred as gas adsorbents for the classic merits of hydrothermal and chemical stabilities, and temperature and high pressure resistance. A large number of carbon members, for instance, activated carbon [13–17], single-walled carbon nanotubes (SWCNTs) [18–20], graphite nanofibers (GNFs) [14,21] and carbon nanohorns [22,23] have been synthesized and accordingly attempted for use in this area. Recently, a new kind of carbon materials named carbon nanoscrolls [24] has attracted our attention. Despite the pristine carbon nanoscrolls are made up of 25–55 layers of carbon with an interlayer spacing of 0.34 nm, the interlayer spacing can be easily controlled by particle intercalation method during the preparation process [25]. Another important characteristic is that carbon nanoscrolls occupy considerable high and fully accessible surface area, with a theoretical value of 2630 m^2/g for individual sheets [24]. These features are potentially advantageous to adsorption storage of methane and carbon dioxide.

To the best of our knowledge, however, there are solely a few research papers reported on carbon nanoscrolls [24–30]. Furthermore, most of the works focus on hydrogen storage by theoretical prediction [28–30]. In 2007, Coluci et al. pioneered the classical grand canonical Monte Carlo (GCMC) simulations to study the hydrogen storage on carbon nanoscrolls [28]. They found that the gravimetric uptake can be doubled to 5.5 wt.% at 150 K and 1 MPa and an expanded interlayer spacing of 0.64 nm. A sequent molecular dynamics study by the same group revealed that at low temperatures significant hydrogen storage is possible, while this capacity is drastically reduced due to thermal energies at higher temperatures [29]. In the same year, Mpourmpakis et al. used a multiscale theoretical approach to investigate the hydrogen storage on carbon nanoscrolls with and without lithium doping [30]. By combining ab initio calculations with GCMC simulations, they found that carbon nanoscrolls with an opening of the spiral structure about 0.7 nm followed by alkali doping gives an uptake of 3 wt.% at ambient temperature and pressure.

On the basis of the previous works, it seems that carbon nanoscrolls with an expansion of interlayer spacing could be very promising materials for gas storage, not only limited to hydrogen. However, to our surprise, we did not find any experimental and theoretical studies related to the adsorption storage of methane and carbon dioxide on this material. Accordingly, we intend to explore adsorption of methane and carbon dioxide in the carbon nanoscroll. The paper is organized as below. First, we present the structural model for isolated and bundled carbon nanoscrolls. Then, we describe the interaction potential model and the details of molecular simulations. Finally, we systematically simulate the storage of methane and carbon dioxide on carbon nanoscrolls by varying operating conditions and structural parameters of material.

2. Theoretical descriptions

2.1. Structure of carbon nanoscrolls

By rolling up a single sheet of graphite into a truncated Archimedean spiral, a unit of carbon nanoscrolls was constructed [26–30], as shown in Fig. 1a. In this study, only armchair nanoscrolls were considered with a chiral vector of (100, 100). Accordingly, the perimeter corresponding to the arc length of $\overline{AC}$ is 42.6 nm. In the simulations, the structural stability of carbon naonoscrolls is not considered, and the innermost radius was fixed at 1.2 nm on the basis of the quantum mechanics calculations [27]. The interlayer spacing is defined as the distance between the two adjacent points *A* and *B* intersected by any radial line and the Archimedean spiral. The isolated nanoscrolls were obtained by duplicating the unit 10 times along the z-direction perpendicular to the paper plane, having a length of 2.46 nm and a number of 4000 carbon atoms. The square and hexagonal arrays for SWCNTs [31] were used to characterize the structure of carbon nanoscrolls bundles, as seen in Fig. 1b and c. The bundles consist of nine and seven isolated carbon nanoscrolls, total 36,000 and 28,000 carbon atoms for square and hexagonal arrays, respectively. To investigate the adsorption in the interstices among nanoscrolls [20,31], a parameter of the van der Waals (VDW) gap was introduced here, which is defined as the distance between the centres of outermost carbon atom layers on two adjacent nanoscrolls. For a specific bundle, we randomly generated the angular orientations of isolated nanoscrolls [28].

2.2. Potential models

For methane molecules, we used an one-site rather than five-site model, because the former produces almost the same results as the latter at the supercritical condition [32]. Furthermore, it takes advantages of less computation cost than the

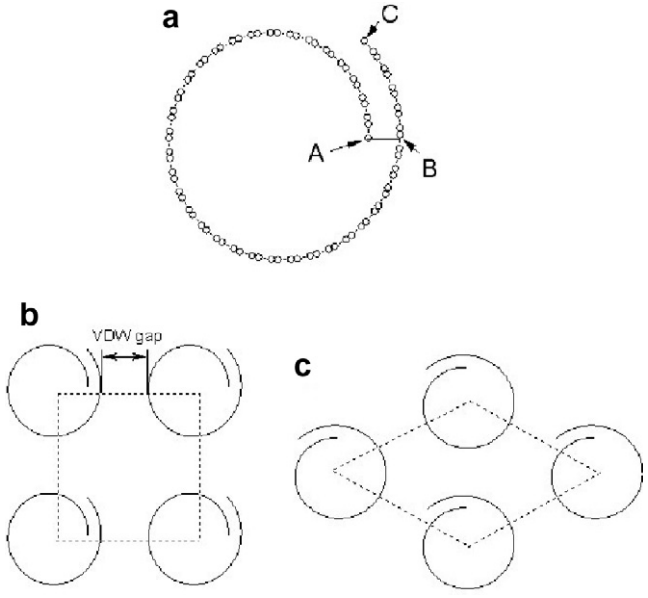

Fig. 1 – Structural model of carbon nanoscrolls: (a) the unit; (b) bundle in square array; (c) bundle in hexagonal array.

latter. Thus, methane molecules are regarded as spherical Lennard-Jones (LJ) particles. The cut-shifted potential was employed to describe the pair interactions between methane molecules and between methane molecule and carbon nanoscrolls [33,34]

$$\phi = \begin{cases} \phi_{LJ}(r) - \phi_{LJ}(r_c) & r < r_c \\ 0 & r \geq r_c \end{cases} \quad (1)$$

where r denotes the inter-site distance, $r_c = 3.5\sigma$ is the cut-off radius with σ being the LJ size parameter. In Eq. (1), $\phi_{LJ}(r)$ represents the full 12–6 LJ potential

$$\phi_{LJ}(r) = 4\varepsilon\left[\left(\frac{\sigma}{r}\right)^{12} - \left(\frac{\sigma}{r}\right)^{6}\right] \quad (2)$$

where ε denotes the LJ energy parameter.

To take into account the quadrapolar effect and linear geometry of carbon dioxide molecule, we used the three-site EPM2 potential model as a three-center LJ plus, a set of partial point charges distributed at three electrostatic sites [1,35]. The fluid–fluid interaction of carbon dioxide is composed of the LJ potential and electrostatic interaction of sites m on molecule i with the site n on molecule j [1]

$$\phi_{ff}(r) = 4\sum_{im}\sum_{jn}\varepsilon_{im,jn}\left[\left(\frac{\sigma_{im,jn}}{r_{im,jn}}\right)^{12} - \left(\frac{\sigma_{im,jn}}{r_{im,jn}}\right)^{6}\right] + \sum_{im}\sum_{jn} \times \frac{q_{im}q_{jn}}{r_{im,jn}} \quad (3)$$

where the subscripts i and j denote different molecules; m and n are the sites on the molecules i and j, respectively. and σ are the energy and size parameters of site–site from the LB combining rule, q is the charge of different sites, is the inter-site distance. The potential between a carbon dioxide molecule and the carbon atoms on nanoscrolls is described by the site-to-site method [1]

$$\phi_{fc}(r) = 4\varepsilon_{fc}\sum_{i=1}^{N_f}\sum_{j=1}^{N_c}\left[\left(\frac{\sigma_{fc}}{r_{ij}}\right)^{12} - \left(\frac{\sigma_{fc}}{r_{ij}}\right)^{6}\right] \quad (4)$$

where r_{ij} is the distance between a site of carbon dioxide molecule and a carbon atom on nanoscrolls, ε_{fc} and σ_{fc} are the cross interaction parameters, N_f and N_c are the site numbers of carbon dioxide molecules and carbon atoms of nanoscrolls, respectively. All the potential parameters used for fluid molecules and carbon nanoscrolls were given in Table 1.

2.3. Simulation details

In the simulation, the structure of the nanoscrolls is assumed to be rigid without geometrical variation. Simulations were independently conducted in a box with the sizes of $12 \times 12 \times 2.46\ nm^3$ for isolated nanoscrolls and $28 \times 28 \times 2.46\ nm^3$ for bundles. We used a standard GCMC technique [33,34] to study the adsorption of methane on carbon nanoscrolls. The modified Bennedict-Webb-Rubin (MBWR) equation of state (EOS) was adopted to convert chemical potential into pressure and to determine the bulk density [36,37]. The calculated bulk density was rigorously verified by the experimental data [38] and the average relative error is less than 1%. Initial configurations of methane molecules were randomly generated without overlaps with the adsorbent.

The adsorption of carbon dioxide molecules in carbon nanoscrolls was studied by the constant pressure Gibbs ensemble Monte Carlo (GEMC) method [1,39,40]. One attracting advantage of the technique is that it uses the pressure of bulk phase as an input parameter to avoid the specification of chemical potential or fugacity in GCMC method, where it is usually be converted to the pressure either through an accurate equation of state (EOS) for fluids or by Widom particle inserting method during the simulation process. In the GEMC method, two simulation cells, one of which stands for the pore phase and the other for the coexisting bulk phase, are performed simultaneously. The total number of particles, N in both cells, the box volume containing nanoscrolls adsorbent, V_P and the temperature, T are fixed in the simulation. A GEMC procedure includes three types of move, namely, particle displacement (including translation and rotation) in both cells with the usual Metropolis scheme, particle exchange to ensure the chemical potential equilibrium between bulk and pore phases, and the random perturbation in the volume of the bulk cell to ensure the bulk pressure is fixed. At the beginning of the simulation, about 4000 of carbon dioxide molecules were generated in the bulk phase. With the process of the simulation, these molecules gradually enter the pore phase under the criteria of the GEMC. The cut-off radius is set to 3.4 nm for the LJ and electrostatic potentials to ensure the electrostatic contribution beyond this cut-off not more than 2% of the total energy by performing an additional simulation in bulk phase with Ewald technique. The acceptance criteria of three trial moves are depicted elsewhere [39,40].

For all the simulations, the periodic boundary conditions were imposed in three directions of the simulation box. A total number of 2×10^7 configurations were generated at each state. The first 1×10^7 moves were discarded to guarantee the equilibrium, and the followed 1×10^7 moves were divided into ten blocks and accumulated for ensemble average. The standard deviation of the properties such as the average number of fluid particles and the total potential energy is estimated to be less than 2%.

Table 1 – Potential parameters for methane, carbon dioxide and carbon nanoscrolls.

Species	Atom	bl (nm)	q (e)	σ (nm)	(ε/k_b) (K)	Ref.
Methane	–	–	–	0.381	148.2	[5]
Carbon dioxide	C	0.0	0.6512	0.2757	28.129	[1,35]
	O	0.1149	−0.3256	0.3033	80.507	–
Nanoscrolls	C	–	–	0.34	28.0	[5,20]

Note: bl is the distance from the interaction site to molecular mass center.

2.4. Calculation of adsorption amount and heat

Because the simulations were carried out in a box that filled with the bulk gas, the storage performance of carbon nanoscrolls was evaluated by the definition of excess adsorption [12]

$$n_{ex} = n_{abs} - \rho_b V_{av} \quad (5)$$

where n_{abs} is the absolute adsorption amount of methane in the simulation box, ρ_b is the bulk density and V_{av} is the available volume to methane molecules. To calculate the V_{av}, a Monte Carlo integration with the reentrant surface definition [41] were performed, where the required size parameter for carbon dioxide was adapted from the one-site potential model [1].

The gravimetric uptake was expressed as the weight ratio of adsorption amount of fluid molecules to carbon atoms on carbon nanoscrolls (mmol/g), while the volumetric uptake is calculated according to the volume of fluid adsorbed at standard temperature and pressure (STP) per volume of nanoscrolls adsorbent (v/v). The volume of carbon nanoscrolls is equivalent to their length in z-direction multiplied by cross-sectional area. By integrating over the region that enclosed by the outermost and second outermost carbon layers, the cross-sectional area A is obtained as follows:

$$A = \int r^2 d\theta = \frac{1}{2}\int_0^{2\pi} (\Delta\theta + r_{out} - 2\pi\Delta)^2 d\theta$$
$$= \frac{4}{3}\Delta^2\pi^3 + 2\Delta(r_{out} - 2\pi\Delta)\pi^2 + (r_{out} - 2\pi\Delta)\pi \quad (6)$$

where r is the polar equation of spiral, $r = \Delta\theta + r_{in}$, r_{in} and r_{out} are the radii of innermost and outermost layers, respectively.

In adsorption studies, the isosteric heat q_{st} is a thermodynamic property that reflects the strength of the interaction between adsorbent and fluid molecules. It is commonly approximated by using multiple isotherms and Clausius–Clapeyron equation [10]

$$q_{st} = -R\frac{d(\ln P)}{d(1/T)} \quad (7)$$

where R, P and T are the universal gas constant, pressure and temperature, respectively. For methane, three adsorption isotherms were selected at 288.15, 298.15 and 308.15 K, while for carbon dioxide they are 273.15, 298.15 and 323.15 K.

3. Results and discussion

3.1. Storage of methane on isolated carbon nanoscrolls

According to the TEM images of carbon nanoscrolls where both isolated and bundled structures had been observed [25], we intend to explore the adsorption behaviour of methane on the isolated one first, and then on the bundles. Fig. 2a shows the adsorption isotherms of methane on isolated carbon nanoscrolls at 298.15 K. We can see that at the interlayer spacing Δ = 0.34 nm, the gravimetric and volumetric uptakes are relatively low, less than 3.0 mmol/g and 129 v/v over the whole pressure range. It means that the pris-

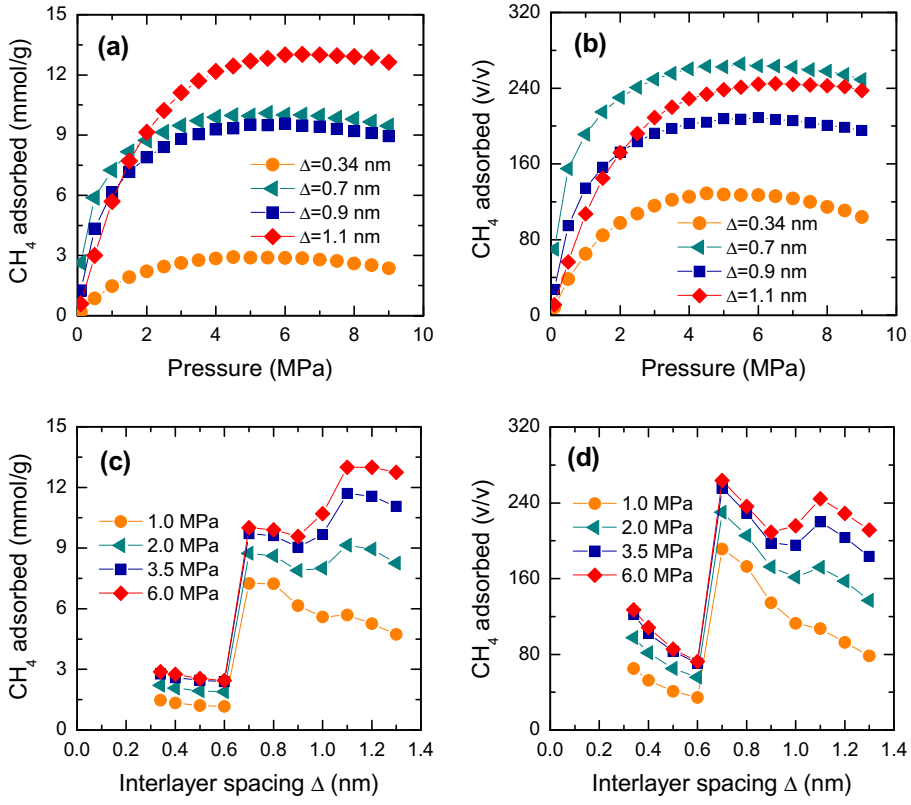

Fig. 2 – Adsorption of methane on isolated carbon nanoscrolls at 298.15 K: (a) gravimetric adsorption isotherms, (b) volumetirc adsorption isotherms, (c) effect of interlayer spacing on gravimetric adsorption, (d) effect of interlayer spacing on volumetric adsorption.

tine carbon nanoscrolls with $\Delta = 0.34$ nm cannot meet the requirement of methane storage at ambient temperature. However, adsorption capacity will be significantly improved once the interlayer spacing is expanded. For instance, at 3.5 MPa and $\Delta = 0.7$ nm, the gravimetric and volumetric uptakes exhibit a 250% and 109% increment, giving a value of 9.7 mmol/g and 255.6 v/v, respectively. A further observation in Fig. 2a reveals that at $P \leqslant 1.5$ MPa, the gravimetric uptake at $\Delta = 0.7$ nm is higher than those at other interlayer spacings, while a greater uptake is obtained at $\Delta = 1.1$ nm in a higher pressure range $P \geqslant 2.5$ MPa. In contrast, the volumetric adsorption always gives the largest uptake at $\Delta = 0.7$ nm in the pressure range studied (Fig. 2b). Obviously, there exists an optimal interlayer spacing for the gravimetric and volumetric adsorption independently. As a consequence, we plotted the variation of storage capacity with interlayer spacing at different pressures in Fig. 2c and d.

For all the curves, the volumetric uptakes decline more quickly with interlayer spacing than the gravimetric uptakes at $\Delta \leqslant 0.6$ nm. This is a consequence of the increase of nanoscrolls volume with interlayer spacing while the vacancy between the carbon layers is too small to accommodate any methane molecules. The observation is consistent with that for hydrogen adsorption in carbon nanoscrolls [30], where an interlayer spacing more than 0.6 nm is needed in the hydrogen physisorption. However, once the interlayer spacing expands from 0.6 to 0.7 nm, sudden jumps of the uptakes are observed for both cases, in which the adsorption takes place among the carbon layers. Interestingly, at a low pressure of 1.0 MPa, only a single peak is found at $\Delta = 0.7$ nm for both cases, but at a higher pressure, a main and second peaks appear at $\Delta = 1.1$ and 0.7 nm for gravimetric uptake but they are in reverse for volumetric uptake. In particular, at 6.0 MPa the maximum uptake can reach 13 mmol/g at $\Delta = 1.1$ nm and 264 v/v at $\Delta = 0.7$ nm, respectively. For gravimetric adsorption, the existence of an optimal interlayer spacing at $\Delta = 1.1$ nm is a consequence of the summation of the interaction with two walls and this effect is practically the same for slit pores (even quantitatively). However, for volumetric adsorption, the optimal interlayer spacing is at $\Delta = 0.7$ nm rather than at $\Delta = 1.1$ nm, because the nanoscrolls at $\Delta = 0.7$ nm have a smaller material volume than that at $\Delta = 1.1$ nm. In summary, under high pressure conditions, it is impossible to achieve the greatest gravimetric and volumetric capacity at a single value of interlayer spacing, simultaneously.

We performed a further analysis at microscopic level by combining local density profiles (Fig. 3) and snapshots (Fig. 4). Fig. 3 shows that the adsorption occurred inside and outside the nanoscrolls would lead to a couple of strong peaks in the local density profile for each interlayer spacing. The snapshots in Fig. 4 also confirm this observation. At $\Delta = 0.34$ nm, the local density between the two peaks is trivial, consistent with the snapshot (Fig. 4a) where no methane molecules are adsorbed in the inner of the carbon layers. In contrast, the local densities at $\Delta = 0.7$ and 1.1 nm show high plateaus between the two peaks, corresponding to one and two completely adsorbed layers in the interlayer space, respectively (Fig. 4b and c). Clearly, these two cases are most efficient for molecule packing, and thus provide a reasonable explanation for the two peaks shown in Fig. 3. It is well known

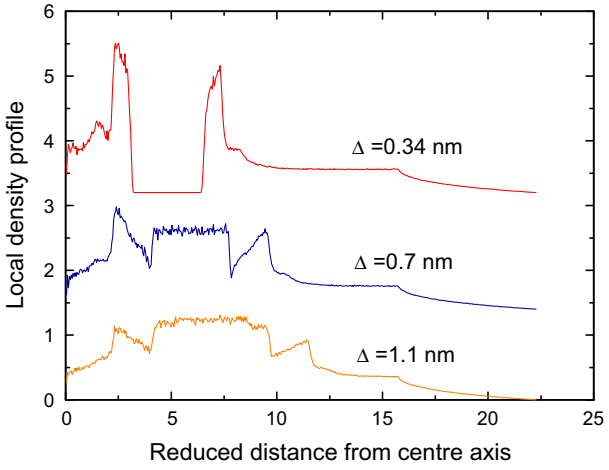

Fig. 3 – Local density profiles of methane on isolated carbon nanoscrolls at 298.15 K and 9.0 MPa. The simulation box in the radial direction was divided into 500 layers and the density of methane located in the range from r^* to $r^* + \Delta r^*$ was collected for ensemble average. The local densities for $\Delta = 0.34$ and 0.7 nm are offset vertically by 3.2 and 1.4, respectively.

that the optimum pore width is about 1.1 nm for methane storage in a slit pore [13,17,19]. From the gravimetric adsorption point of view, it agrees well with the carbon nanoscrolls at $\Delta = 1.1$ nm. However, if the volumetric definition is used, the optimal pore size may shift from the formation of the two molecule layers to the monolayer.

The isosteric heat is shown in Fig. 5 as a function of methane adsorption amount. At $\Delta = 1.1$ nm, the isosteric heat gradually increases with the loading, which gives the similar trend to the activated carbon at the pore width of 1.14 nm and 298 K [13]. Furthermore, the isosteric heat at zero coverage is 12.1 kJ/mol, which is among the range of 11.8–13.3 kJ/mol for activated carbon. Different from $\Delta = 1.1$ nm, the isosteric heat at $\Delta = 0.34$ nm rises drastically in a narrow loading region, while at $\Delta = 0.7$ nm the isosteric heat first levels off below the loading of 4 mmol/g, then exhibits a slight maximum of 23.7 kJ/mol at the loading of 5.2 mmol/g, and finally levels off again at high loadings. In fact, the variation of the isosteric heat comes mostly from the intermolecular (methane–methane) interaction which gives different values as a function of the density of adsorbed methane. As suggested in the literature [19], an ideal adsorbent for methane storage exhibits not only an optimum isosteric heat of 18.8 kJ/mol at 298 K, but also is energetically homogeneous. Accordingly, the carbon nanoscrolls with $\Delta = 1.1$ nm is a good candidate adsorbent, not only because the greatest adsorption amount is obtained at this interlayer spacing, but also because the isosteric heat is slowly increased with loading and the average value of 15.7 kJ/mol is also close to the optimum one.

3.2. *Storage of methane on carbon nanoscrolls bundles*

The previous simulations for SWCNTs indicate that at the optimal VDW gap of 0.8 nm, about 60% of the total amount can be adsorbed in the interstices of tubes [20]. With the same

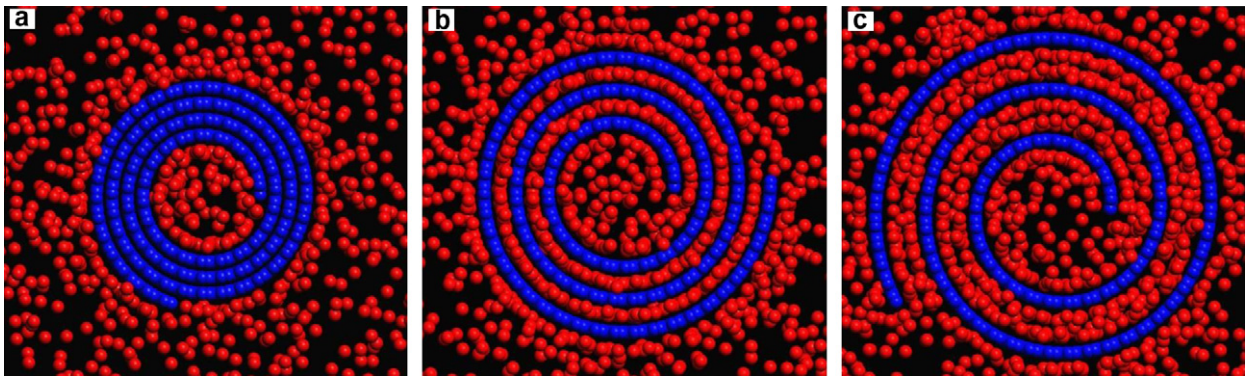

Fig. 4 – Snapshots of methane adsorbed on isolated carbon nanoscrolls at 298.15 K and 9.0 MPa: (a) Δ = 0.34 nm; (b) Δ = 0.7 nm; (c) Δ = 1.1 nm. The blue and red spheres denote carbon atom on nanoscrolls and methane molecule, respectively. (For interpretation of the references to colour in this figure legend, the reader is referred to the web version of this article.)

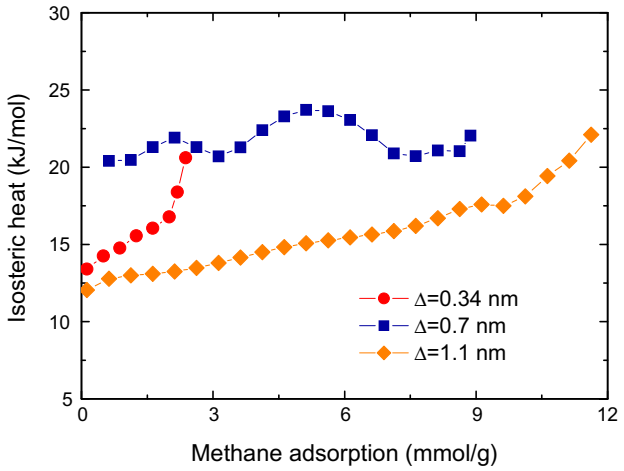

Fig. 5 – Isosteric heat versus methane adsorption amount on isolated carbon nanoscrolls.

expectation, we examined the uptakes on the carbon nanoscrolls bundles with the optimized interlayer spacing Δ = 0.7 and 1.1 nm. However, as seen in Fig. S1 (see Supporting Information), any remarkable enhancement of uptakes are not found with the decrease of VDW gap from 0.9 to 0.34 nm. This is because adsorption on external surface has already been taken into account for the isolated carbon nanoscrolls, while it was not considered in the literature [20]. The snapshots in Fig. S2 (see Supporting Information) also confirm this conclusion.

The remaining factor that can influence adsorption is the innermost radius, if the nanoscroll structures are stable. Fig. S3 (see Supporting Information) shows that all the uptakes increase slightly with innermost radius at Δ = 0.34 nm, while at Δ = 0.7 and 1.1 nm, the decrease of innermost radius will not affect the gravimetric uptake pronouncedly, but is slightly advantageous to the volumetric adsorption. This is because at Δ = 0.34 nm, the adjacent carbon layer can also make a contribution to the adsorption inside the innermost space. However, at the expanded interlayer spacing of Δ = 0.7 and 1.1 nm, the contribution become gradually trivial due to the decay of LJ potential interaction between carbon layer and fluid molecules.

3.3. *Capture of carbon dioxide on isolated carbon nanoscrolls*

Based on the above simulations for methane adsorption, we concluded that the effects of VDW gap and innermost radius on adsorption are trivial. Therefore, we did not make effort to explore the effect of these variables on carbon dioxide storage. Instead, we only paid our attentions to the adsorption of carbon dioxide on isolated carbon nanoscrolls.

Fig. 6 shows the adsorption isotherms of carbon dioxide at three temperatures of 273.15, 298.15 and 323.15 K and different interlayer spacings. The simulations at 273.15 and 298.15 K were confined no more than the saturated vapor pressures of 3.47 and 6.44 MPa, respectively. At 298.15 K, the loading of carbon dioxide can reach 28.97 mmol/g at 5.0 MPa and Δ = 1.5 nm, approaching to that of Mg-IRMOF1 (30.58 mmol/g) and Be-IRMOF1 (33.12 mmol/g) where the adsorption was greatly improved by doping metal cation [42]. More importantly, it is higher than 3.5 times than that of (10, 10) SWCNTs with a diameter of 1.356 nm [42], although both of them belong to the same carbonaceous family. Nevertheless, if the interlayer spacing of carbon nanoscrolls is not expanded, the capacity is only comparable to that of SWCNTs, exhibiting an uptake of 7.47 mmol/g. As expected, the uptake at 273.15 K is always the highest among the three temperatures, approximating to 34.6 mmol/g at 3.0 MPa and Δ = 1.5 nm. By contrast, if the temperature is raised to 323.15 K, the uptake will fall down to 22.3 mmol/g at Δ = 1.5 nm even at a high pressure of 9.0 MPa.

The influence of these factors on adsorption was further analyzed by the adsorption data (see Fig. S4) and the snapshots of carbon dioxide molecules at 3.0 MPa (see Fig. 7). It is shown that a lower temperature and wider interlayer spacing obviously make the adsorption better, giving a 260–310% and 90–150% increment, respectively. From the snapshots in Fig. 7a and b, we find that the increased uptake at Δ = 1.5 nm mostly arises from additional adsorption occurred in the interlayer space, whereas it is prohibited at Δ = 0.34 nm. Differently, at Δ = 1.5 nm (see Fig. 7c and d), the volume between the interlayer spacings had already been filled with carbon dioxide molecules for both temperatures. In this case, the uptake increment by decreasing temperature is mainly owing to the densification of carbon dioxide in the space surrounded by the innermost nanoscrolls sheet.

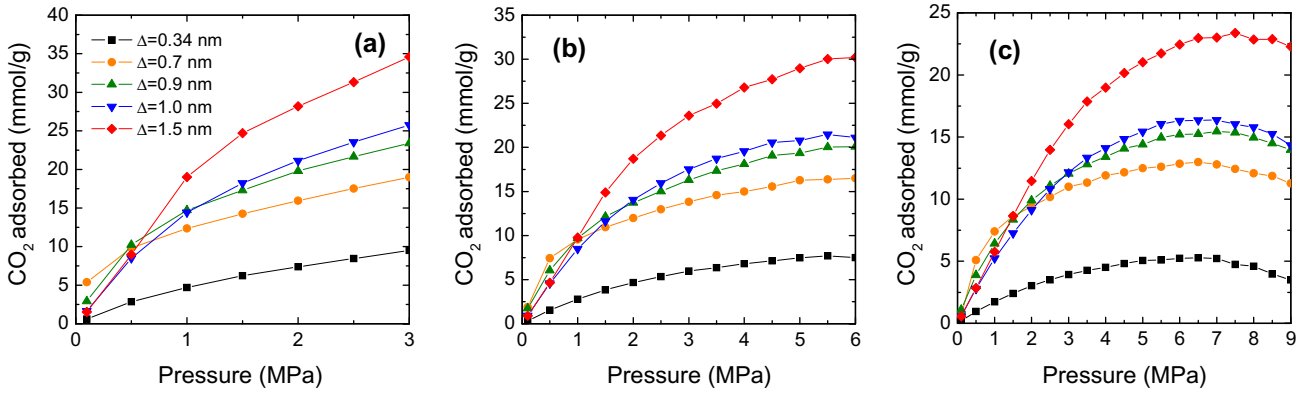

Fig. 6 – Adsorption isotherms of carbon dioxide on isolated carbon nanoscrolls (a) 273.15 K, (b) 298.15 K, (c) 323.15 K.

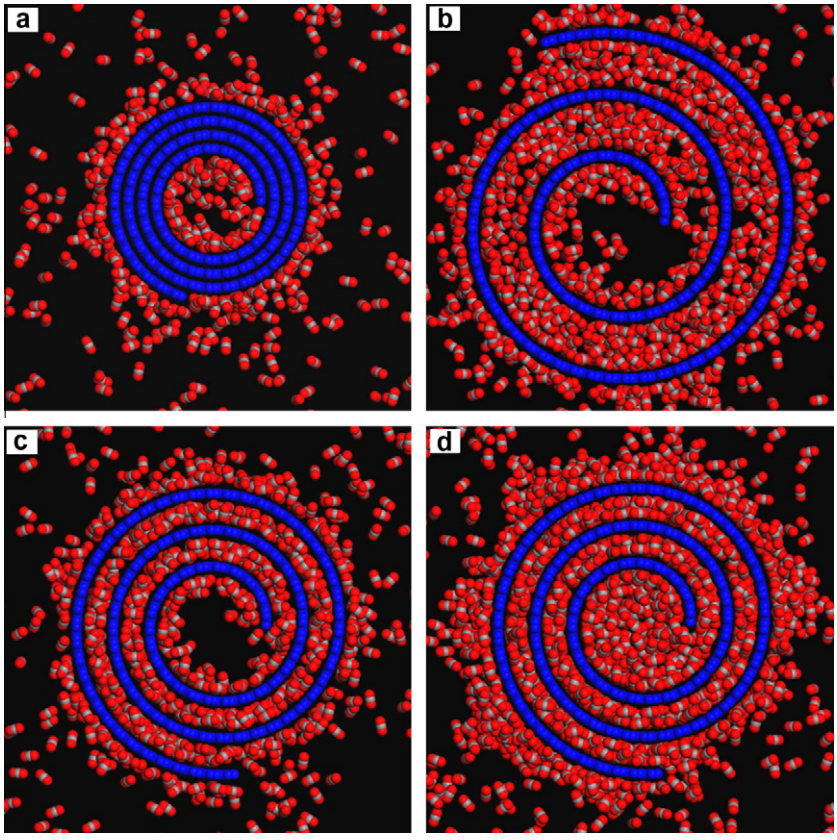

Fig. 7 – Snapshots of carbon dioxide adsorbed on isolated carbon nanoscrolls at 3.0 MPa, (a) 323.15 K and Δ = 0.34 nm; (b) 323.15 K and Δ = 1.5 nm; (c) 323.15 K and Δ = 0.9 nm; (d) 273.15 K and Δ = 0.9 nm.

Due to the adsorption isotherm at 323.15 K exhibiting a maximum for each interlayer spacing (see Fig. 6), we further plotted the optimal pressure and corresponding maximum uptake at the temperature in Fig. 8. It is seen that the optimal pressure slightly increases with interlayer spacing, concentrating on the range of 6.5–7.5 MPa, compared to the rapid ascending of maximum uptake. Fig. 9 shows the isosteric heat of carbon dioxide at different interlayer spacings. Depending on the uptake, the isosteric heat varies in a wide range of 8–23 kJ/mol. Furthermore, the ascending rate of isosteric heat gradually becomes moderate when the interlayer spacing is expanded from 0.34 to 1.5 nm.

4. Conclusion

Adsorption storage of methane and capture of carbon dioxide on isolated and bundled carbon nanoscrolls have been investigated by GCMC and GEMC simulations. The isolated carbon nanoscrolls are constructed by rolling up a single sheet of graphite into a truncated Archimedean spiral. The structures of the bundles are characterized by the hexagonal and square arrays of isolated nanoscrolls. We have systematically investigated the effects of the pressure, temperature, interlayer spacing, VDW gap and innermost radius on the adsorption of methane and carbon dioxide on carbon nanoscrolls. The

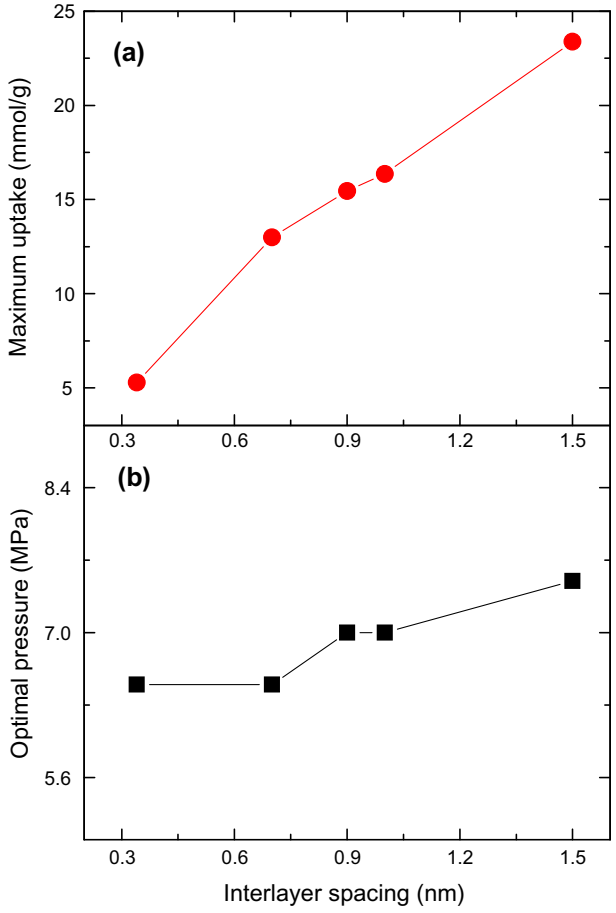

Fig. 8 – Dependence of optimal pressure and the corresponding maximum uptake of carbon dioxide on isolated carbon nanoscrolls at 323.15 K on interlayer spacing. (a) Maximum uptake; (b) optimal pressure.

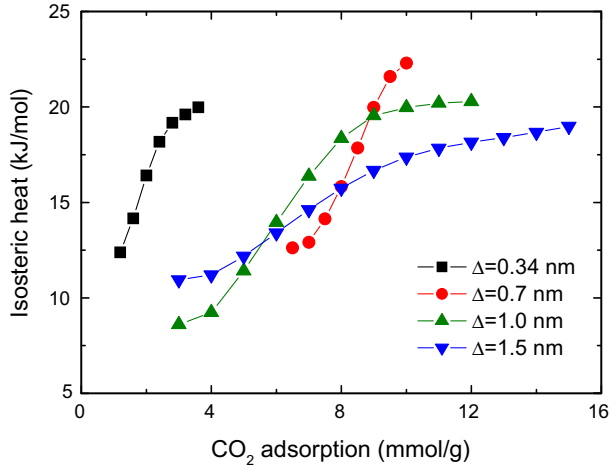

Fig. 9 – Isosteric heat versus carbon dioxide adsorption amount on isolated carbon nanoscrolls.

VDW gap and innermost radius have no evident influences on the adsorption, while interlayer spacing plays the most important role in the adsorption. By further analysing the local density profiles and snapshots of methane, we find that optimal pore size for methane storage is achieved in double adsorbed layers. We recommend the carbon nanoscrolls with Δ = 1.1 nm as a candidate adsorbent for methane storage, not only for the greatest uptake, but also because the average isosteric heat of 15.7 kJ/mol is close to the optimum one.

As to carbon dioxide, both interlayer spacing and temperature have distinct effects on its adsorption capacity. For example, although a high temperature of 323.15 K is not good for adsorption, the uptake of carbon dioxide at 3.0 MPa presents a threefold increase due to the expansion of interlayer spacing from 0.34 to 1.5 nm. Similarly, when the temperature is lowered from 323.15 to 273.15 K, the uptake could be enhanced doubly for different interlayer spacings. Especially, at Δ = 1.5 nm, the adsorbent exhibits a quite high uptake of 30.21 mmol/g at 298.15 K and 6.0 MPa, and 34.6 mmol/g at 273.15 K and 3.0 MPa, respectively. It is worthwhile to note that the adsorption is not saturated yet for both temperatures, indicating a latent probability to improve the storage capacity. In view of the fact that the adsorption of carbon dioxide with a quadrapolar moment would be definitely favoured on polar adsorbents, modification of materials by intercalating functional groups into interlayer spaces and loading the active species on the surface might be a good choice for such applications. In conclusion, this work suggests that carbon nanoscrolls with an expansion of interlayer spacing could be a suitable material for methane and carbon dioxide storage at room temperature. It is expected that our simulations will be verified experimentally in the future.

Acknowledgements

This work is supported by the NSF of China (No. 20806003, 20736002), National Scientific Research Funding (ZD0901), the Young Scholars Fund of Beijing University of Chemical Technology (BUCT) and Guangzhou Center for Gas Hydrate Research, Chinese Academy of Sciences (No.CASHYD0907s3). We thank the Chemical Grid Project of BUCT for providing computational platform.

Appendix A. Supplementary data

Supplementary data associated with this article can be found, in the online version, at doi:10.1016/j.carbon.2010.06.038.

REFERENCES

[1] Peng X, Zhao JS, Cao DP. Adsorption of carbon dioxide of 1-site and 3-site models in pillared clays: a gibbs ensemble Monte Carlo simulation. J Colloid Inter Sci 2007;310:391–401.
[2] Benson SM, Orr JFM. Carbon dioxide capture and storage. Mrs Bulletin 2008;33:303–5.
[3] Peng X, Wang WC. Molecular simulation for the chemical equilibrium of methane steam reforming in slit pores. Chem J Chinese Univ 2006;27:1530–4.
[4] Peng X, Wang WC, Xue RS, Shen ZM. Adsorption separation of CH_4/CO_2 on mesocarbon microbeads: experiment and modeling. AIChE J 2006;52:994–1003.
[5] Peng X, Cao DP, Wang WC. Heterogeneity characterization of ordered mesoporous carbon adsorbent CMK-1 for methane

and hydrogen storage: GCMC simulation and comparison with experiment. J Phys Chem C 2008;112:13024–36.
[6] Peng X, Cao DP, Wang WC. Computational characterization of hexagonally ordered carbon nanopipes CMK-5 and structural optimization for H_2 storage. Langmuir 2009;25:10863–72.
[7] Cao DP, Lan JH, Wang WC, Smit B. Li-doped 3D covalent organic frameworks: high capacity hydrogen storage materials. Angew Chem Int Ed 2009;48:4730–3.
[8] Furukawa H, Yaghi OM. Storage of hydrogen, methane, and carbon dioxide in highly porous organic frameworks for clean energy applications. J Am Chem Soc 2009;131:8875–83.
[9] Lan JH, Cao DP, Wang WC. High uptake of methane in Li-doped 3D covalent-organic frameworks. Langmuir 2010;26:220–6.
[10] Ma S, Sun D, Simmons JM, Collier CD, Yuan D, Zhou HC. Metal–organic framework from an anthracene derivative containing nanoscopic cages exhibiting high methane uptake. J Am Chem Soc 2008;130:1012–6.
[11] Eddaoudi M, Kim J, Rosi N, Vodak D, Wachter J, Okeeffe M, et al. Systematic design of pore size and functionality in isoreticular MOFs and their application in methane storage. Science 2002;295:469–72.
[12] Düren T, Sarkisov L, Yaghi OM, Snurr RQ. Design of new materials for methane storage. Langmuir 2004;20:2683–9.
[13] Matranga KR, Myers AL, Glandt ED. Storage of natural gas by adsorption on activated carbon. Chem Eng Sci 1991;47:1569–79.
[14] Jiang SY, Zollweg JA, Gubbins KE. High-pressure adsorption of methane and ethane in activated carbon and carbon fibers. J Phys Chem 1994;98:5709–13.
[15] Lozano-Castelló D, Cazorla-Amorós D, Linares-Solano A, Quinn DF. Influence of pore size distribution on methane storage at relatively low pressure: preparation of activated carbon with optimum pore size. Carbon 2002;40:989–1002.
[16] Vishnyakov A, Ravikovitch P, Neimark AV. Molecular level models for CO_2 sorption in nanopores. Langmuir 1999;15:8736–42.
[17] Cao DP, Wang WC, Shen ZG, Chen JF. Determination of pore size distribution and adsorption of methane and CCl_4 on activated carbon by molecular simulation. Carbon 2002;40:2359–65.
[18] Kowalczyk P, Solarz L, Do DD, Samborski A, MacElroy JM. Nanoscale tubular vessels for storage of methane at ambient temperatures. Langmuir 2006;22:9035–40.
[19] Bhatia S, Myers AL. Optimum conditions for adsorptive storage. Langmuir 2006;22:1688–700.
[20] Cao DP, Zhang XR, Chen JF, Wang WC, Yun J. Optimization of single-walled carbon nanotube arrays for methane storage at room temperature. J Phys Chem B 2003;107:13286–92.
[21] Alcañiz-Monge J, Casa-Lillo MA, Cazorla-Amorós D, Linares-Solano A. Methane storage in activated carbon fibres. Carbon 1997;35:291–7.
[22] Bekyarova E, Murata K, Yudasaka M, Kasuya D, Iijima S, Tanaka H, et al. Single-wall nanostructured carbon for methane storage. J Phys Chem B 2003;107:4681–4.
[23] Murata K, Hashimoto A, Yudasaka M, Kasuya D, Kaneko K, Iijima S. The use of charge transfer to enhance the methane-storage capacity of single-walled, nanostructured carbon. Adv Mater 2004;16:1520–2.
[24] Viculis LM, Mack JJ, Kaner RB. A chemical route to carbon nanoscrolls. Science 2003;299. 1361–1.
[25] Savoskin MV, Mochalin VN, Yaroshenko AP, Lazareva NI, Konstantinova TE, Barsukov IV, et al. Carbon nanoscrolls produced from acceptor-type graphite intercalation compounds. Carbon 2007;45:2797–800.
[26] Braga SF, Coluci VR, Legoas SB, Giro R, Galvão DS, Baughman RH. Structure and dynamics of carbon nanoscrolls. Nano Lett 2004;4:881–4.
[27] Chen Y, Lu J, Gao ZX. Structural and electronic study of nanoscrolls rolled up by a single graphene sheet. J Phys Chem C 2007;111:1625–30.
[28] Coluci VR, Braga SF, Baughman RH, Galvão DS. Prediction of the hydrogen storage capacity of carbon nanoscrolls. Phys Rev B 2007;75:125404–6.
[29] Braga SF, Coluci VR, Baughman RH, Galvão DS. Hydrogen storage in carbon nanoscrolls: an atomistic molecular dynamics study. Chem Phys Lett 2007;441:78–82.
[30] Mpourmpakis G, Tylianakis E, Froudakis GE. Carbon nanoscrolls: a promising material for hydrogen storage. Nano Lett 2007;7:1893–7.
[31] Zhang XR, Cao DP, Chen JF. Hydrogen adsorption storage on single-walled carbon nanotube arrays by a combination of classical potential and density functional theory. J Phys Chem B 2003;107:4942–50.
[32] Do DD, Do HD. Evaluation of 1-site and 5-site models of methane on its adsorption on graphite and in graphitic slit pores. J Phys Chem B 2005;109:19288–95.
[33] Frenkel D, Smit B. Understanding molecular simulations. New York: Academic Press; 2002.
[34] Allen MP, Tildesley DJ. Computer simulation of liquids. Oxford: Clarendon Press; 1987.
[35] Harris JG, Yung KH. Carbon dioxide liquid–vapor coexistence curve and critical properties as predicted by a simple molecular model. J Phys Chem 1995;99:12021–4.
[36] Nicolas JJ, Gubbins KE, Streett WB, Tildesley GJ. Equation of state for the Lennard-Jones fluid. Mol Phys 1979;37:1429–54.
[37] Johnson JK, Zollweg JA, Gubbins KE. The Lennard-Jones equation of state revisited. Mol Phys 1993;78:591–618.
[38] Kowalczyk P, Tanaka H, Kaneko K, Terzyk AP, Do DD. Grand canonical Monte Carlo simulation study of methane adsorption at an open graphite surface and in slitlike carbon pores at 273 K. Langmuir 2005;21:5639–46.
[39] Mcgrother SC, Gubbins KE. Constant pressure gibbs ensemble Monte Carlo simulations of adsorption into narrow pores. Mol Phys 1999;97:955–65.
[40] Panagiotopoulos AZ. Adsorption and capillary condensation of fluids in cylindrical pores by Monte Carlo simulation in the gibbs ensemble. Mol Phys 1987;62:701–19.
[41] Thomson KT, Gubbins KE. Modeling structural morphology of microporous carbons by reverse Monte Carlo. Langmuir 2000;16:5761–73.
[42] Babarao R, Jiang JW. Molecular screening of metal–organic frameworks for CO_2 storage. Langmuir 2008:6270–8.